research article

Semi-supervised planning method for breast electronic tissue compensation treatments based on breast radius and separation

Alexander R. Podgorsak[1,2], Lalith K. Kumaraswamy[1,2]

[1] State University of New York at Buffalo, Department of Medical Physics, Buffalo, New York, United States
[2] Roswell Park Comprehensive Cancer Center, Department of Radiation Medicine, Buffalo, New York, United States

Radiol Oncol 2021; 55(1): 106-115.

Received 24 July 2020
Accepted 19 October 2020

Correspondence to: Alexander R. Podgoršak, Ph.D., 8052 Clinical Translational Research Center, 875 Ellicott Street, Buffalo, New York 14203. E-mail: arpodgor@buffalo.edu

Disclosure: No potential conflicts of interest were disclosed.

Background. The aim of the study was to develop and assess a technique for the optimization of breast electronic tissue compensation (ECOMP) treatment plans based on the breast radius and separation.

Materials and methods. Ten ECOMP plans for 10 breast cancer patients delivered at our institute were collected for this work. Pre-treatment CT-simulation images were anonymized and input to a framework for estimation of the breast radius and separation for each axial slice. Optimal treatment fluence was estimated based on the breast radius and separation, and a total beam fluence map for both medial and lateral fields was generated. These maps were then imported into the Eclipse Treatment Planning System and used to calculate a dose distribution. The distribution was compared to the original treatment hand-optimized by a medical dosimetrist. An additional comparison was performed by generating plans assuming a single tissue penetration depth determined by averaging the breast radius and separation over the entire treatment volume. Comparisons between treatment plans used the dose homogeneity index (HI; lower number is better).

Results. HI was non-inferior between our algorithm (HI = 12.6) and the dosimetrist plans (HI = 9.9) (p-value > 0.05), and was superior than plans obtained using a single penetration depth (HI = 17.0) (p-value < 0.05) averaged over the 10 collected plans. Our semi-supervised algorithm takes approximately 20 seconds for treatment plan generation and runs with minimal user input, which compares favorably with the dosimetrist plans that can take up to 30 minutes of attention for full optimization.

Conclusions. This work indicates the potential clinical utility of a technique for the optimization of ECOMP breast treatments.

Key words: electronic compensation; dose homogeneity index; plan optimization

Introduction

It is estimated that approximately 276,480 new cases of invasive breast cancer will be diagnosed in women in the United States by the end of 2020.[1] One of the techniques used for breast radiation therapy employs two electronically compensated tangent x-ray fields. Such a technique has been found to minimize irradiation of the surrounding lung and cardiac tissue, while improving the homogeneity of the delivered dose within the breast.[2-4] This is important as it is reported that women treated for breast cancer have higher incidence of coronary artery disease and myocardial infarction.[5-7] Additionally, dose inhomogeneity reduction has been shown to reduce adverse effects such as acute radiation toxicity, particularly in women with large breast size.[8,9]

Electronic compensation (ECOMP) is a forward-planned intensity modulated radiation therapy technique which can account for variation in the breast size and shape in both the anterior-posterior

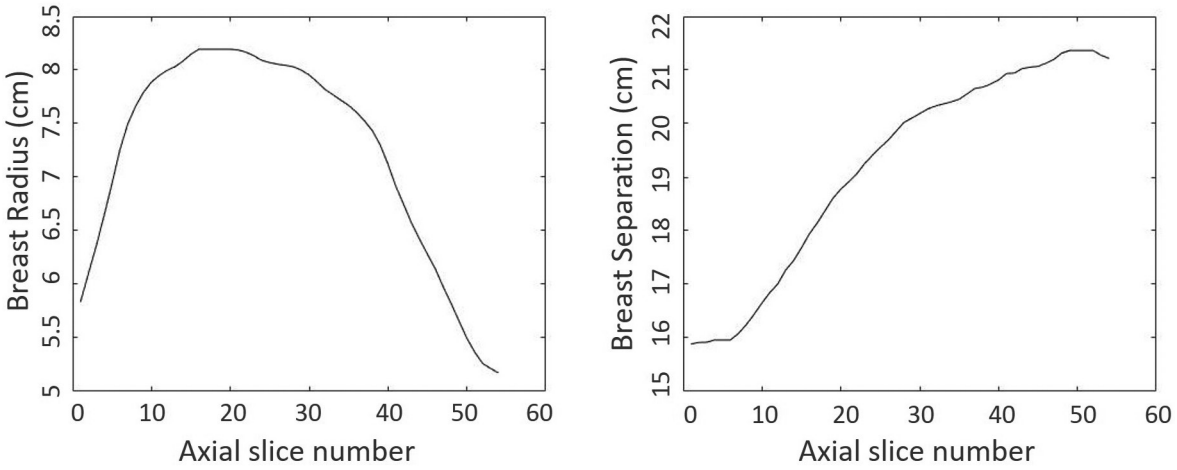

FIGURE 1. Left shows how the breast radius varies in the cranio-caudal direction, right shows how the breast separation varies in the cranio-caudal direction for the same collected patient breast.

and cranio-caudal direction.[10-14] It achieves its improvement in dose homogeneity through dynamic multi-leaf collimator motion. Within the Eclipse (Varian Medical Systems, Palo Alto, United States) treatment planning software (TPS), the irregular compensation surface is defined by a transmission penetration depth (TPD). The TPD is the point along every ray in the field that tissue compensation occurs. If the TPD is reduced, the compensation surface is moved closer to the surface of the breast. Clinically, the TPD is currently selected based on prior knowledge of the treatment planner. Dose profiles are computed within the TPS, and the homogeneity is improved via manual editing of the x-ray fluence maps. This can be a time-consuming process, with large variability between users depending on the skill or experience of the planner.

Published work exists which attempted to correlate the size and shape of the breast to the TPD which yielded the most homogenous dose distribution. Friend *et al.* reported the use of a constant TPD rule depending on breast separation, TPD of 40% if separation is greater than 24 cm, TPD of 50% otherwise.[15] Emmens and James reported the use of smaller TPD with larger breast separation producing a more homogenous dose distribution, yet the full breast volume should be used to attain the most homogenous distribution.[11] These works used a single TPD for all axial breast slices, ignoring the variation in breast size and shape in the cranio-caudal direction. Alghufaili *et al.* correlated the full contour of the breast to the optimal TPD in-terms of achieving a homogenous dose distribution.[16] Three TPDs were output for three regions of the breast (superior, middle, inferior) using the average breast separation and radius in those regions. Our work looks to extend this idea, but use the breast size and shape in *each* axial slice to determine the optimal TPD slice-by-slice.

Materials and methods

Figure 1 shows how the breast radius and separation may change in the cranio-caudal direction for an example patient. Figure 2 shows the hand-calculated optimal TPD over each axial slice in the cranio-caudal direction using the model proposed

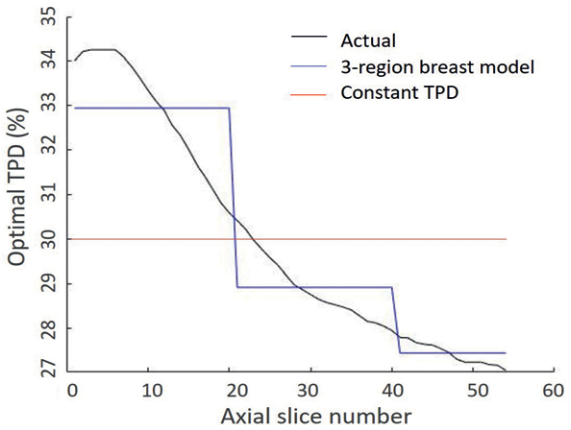

FIGURE 2. Variation in the optimal transmission penetration depth (TPD) over all slices in the cranio-caudal direction compared with the TPD considering a constant TPD or a TPD using the three-region breast approach.

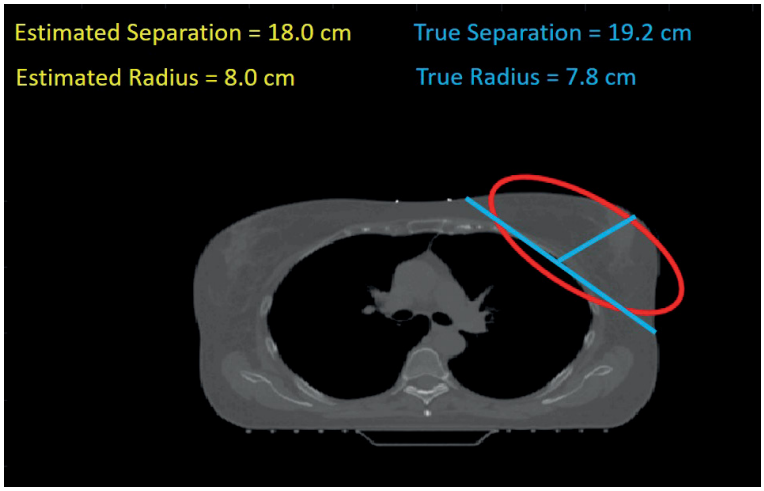

FIGURE 3. CT-simulation axial slice with fitted ellipse (red) and breast radius and separation estimation (yellow) and hand-measurement (blue) of left breast overlaid. Included is the location of the hand measurement for radius and separation in blue.

by Alghufaili, compared with averaging the optimal TPD considering one (constant TPD) and three breast regions. Attempting to select a single or few optimal TPDs over the entire cranio-caudal direction is difficult. With this variation in breast shape and size, and the optimal TPD in the cranio-caudal direction, it seems likely that improvements in ECOMP treatment planning may be realized with a higher-resolution correlation of breast shape and size to the optimal x-ray beam fluence. We look to do this optimal TPD selection with a weakly supervised framework that will estimate the breast separation and radius from input CT-simulation data.

To this end, 10 ECOMP breast plans for 10 breast cancer patients delivered at our institute with a Varian Trilogy LINAC and millennium model 120 multi-leaf collimators were retrospectively collected. CT-simulation data were anonymized for each patient and used to develop our semi-supervised framework for measurement of breast size and separation. Two left-sided and 1 right-sided treatment were used for hand-measurement of the breast separation and radius at each axial location within the treatment volume determined by the placement of superior and inferior markers prior to simulation. It should be noted that a breath hold technique was employed in the left-sided breast cases, both during imaging and treatment. We defined breast separation as the distance along the posterior edge of the breast, and breast radius as the distance from the chest wall to the anterior apex of the breast. Hand measurements were used to assess the accuracy of the semi-supervised breast separation and radius measurement framework.

The first step of the framework is the identification of medial and ipsilateral platinum markers placed prior to CT-simulation. Two square regions are required as input for marker identification. That is the only user supervision the algorithm requires. If the medial marker is found to be to the right of the ipsilateral marker (by x-position), it is a left-sided treatment, otherwise it is a right-sided treatment. A vector is created connecting the medial and ipsilateral markers, extrapolated out to the image boundary, and all image structure beneath the vector is removed from the image data leaving only the targeted breast. An ellipse is fitted to the remaining breast structure using the elliptical Hough transform.[17] The major axis of the fitted ellipse is the estimated breast separation; half of the minor axis is the estimated breast radius. Figure 3 shows an example axial CT-simulation slice with the fitted ellipse and the estimated (yellow) and hand-measured (blue) separation and radius measurement in cm overlaid. For each axial slice in the three breast volumes, the hand-measured separation and radius were compared with the automatically estimated separation and radius using the average percent difference between them.

Previous work has correlated the breast separation and radius to the TPD which will yield the most homogenous dose distribution.[11,15,16] The TPS is still required to compute the fluence profile to deliver the prescribed TPD. We looked to correlate the breast size and shape to that optimal fluence profile, such that the x-ray fluence map needed to achieve the most homogenous dose could be attained without the use of the TPS. To do this, uniform semi-elliptical phantoms simulating axial slices of the breast with varying separation and radius ranging from a separation of 12 cm to 24 cm and a radius of 5 cm to 12 cm were generated. These phantoms were input to Eclipse TPS, and the TPD was set in accordance with the model proposed by Alghufaili *et al*.[16] The TPS was used to measure the x-ray fluence needed to deliver the homogenous dose profile, and correlate it with the breast size and shape. A mathematical model computing the optimal fluence as a function of breast separation and radius was acquired using a least-squares minimization bilateral fitting to the individual fluence measurements. This model can then be used to compute a mapping of the x-ray fluence at the surface of the breast needed to deliver the most homogenous dose, across all axial slices in the treatment volume. It is important to note that this model is dependent on beam energy. As each ray passes through the breast volume, we

assumed exponential drop-off of the fluence governed by the Beer-Lambert-Bouguer Law.[18-20] In this way, we created 2D x-ray fluence maps needed to deliver the most homogenous dose profile, considering each axial slice in the treatment volume, using a semi-supervised processing framework.

The 10 retrospectively collected ECOMP breast plans were re-planned within Eclipse using x-ray fluence maps generated with our proposed semi-supervised framework. The resultant dose distributions were compared with those from the original plans created and optimized by an experienced dosimetrist. Two additional comparisons were carried out with plans generated in Eclipse, the first by assuming a single TPD determined over the entire treatment volume (current model in Eclipse TPS), and no manual editing of the fluence maps to correct any dose inhomogeneities. The second is using Alghufaili's three-region breast model, where three TPD's are used, the optimal TPD for the superior, medial, and inferior portions of the treatment volume. Quantitative comparison between the four plans across the ten patients used the dose homogeneity index (HI, lower is better)[21], mathematically described in Equation 1 as

$$[\text{eq. 1}] \quad HI = \frac{D_2 - D_{98}}{D_p} \times 100\%$$

where D_2 and D_{98} represent doses to 2% and 98% of the PTV respectively, and D_p represents the prescription dose, along with Pearson correlation coefficients[22], and single-tailed heteroscedastic *t*-tests to assess the significance of any differences between plans (p-value < 0.05). Our goal was to achieve a more homogenous dose profile using our semi-supervised algorithm compared with the use of a single TPD over all axial slices in the treatment volume or the 3-region breast model of Alghufaili, and to achieve a statistically non-inferior dose homogeneity compared with the dosimetrist treatment plans. Our institute places constraints on ECOMP plans which mandate global maximum dose less than 108% the prescription and treatment volume dose greater than 95% the prescription. We compared how each of the four techniques created plans which met these dose constraints or otherwise.

The weakly-supervised breast radius and separation estimation process, fitting of the x-ray beam fluence to the mathematical models, and statistical analyses were all done in MATLAB.

Results

Treatment plans were generated in around 20 seconds by our proposed algorithm. This number includes the time it takes for breast radius and separation estimation, and compares well with the medical dosimetrist plans which can take up to 30 minutes due to the iterative and manual process of editing the fluence maps to bring the generated plans within institutional dose constraints. It is also important to note that our proposed algorithm requires much less user input than the fully-supervised forward-planned iterative method, indicating an improvement in the clinical workflow.

TABLE 1. Agreement between breast radius and separation hand-measurements and automatic algorithm measurement in centimeter (cm) difference and percent difference

Radius		
Number	**% Difference**	**Difference (cm)**
1	9.6 [9.3–9.9]	0.70 [0.68–0.72]
2	6.2 [5.7–6.7]	0.40 [0.39–0.41]
3	22.0 [21.5–22.5]	1.00 [0.98–1.02]
Average	12.6 [10.4–14.8]	0.69 [0.59–0.79]
Separation		
Number	**% Difference**	**Difference (cm)**
1	6.1 [5.0–7.2]	1.13 [1.11–1.15]
2	4.2 [4.1–4.3]	0.71 [0.68–0.74]
3	5.3 [5.1–5.5]	0.91 [0.71–1.11]
Average	5.2 [5.1–5.3]	0.92 [0.79–1.05]

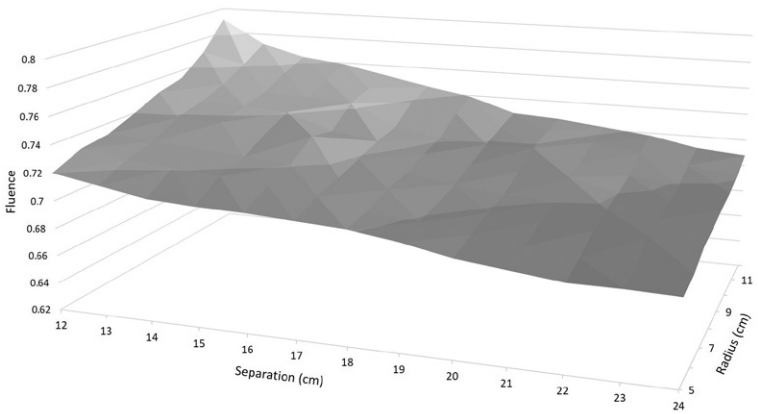

FIGURE 4. Correlation between breast separation and radius with the x-ray fluence needed to deliver homogenous dose distribution to the breast treatment volume using a 6 MV beam.

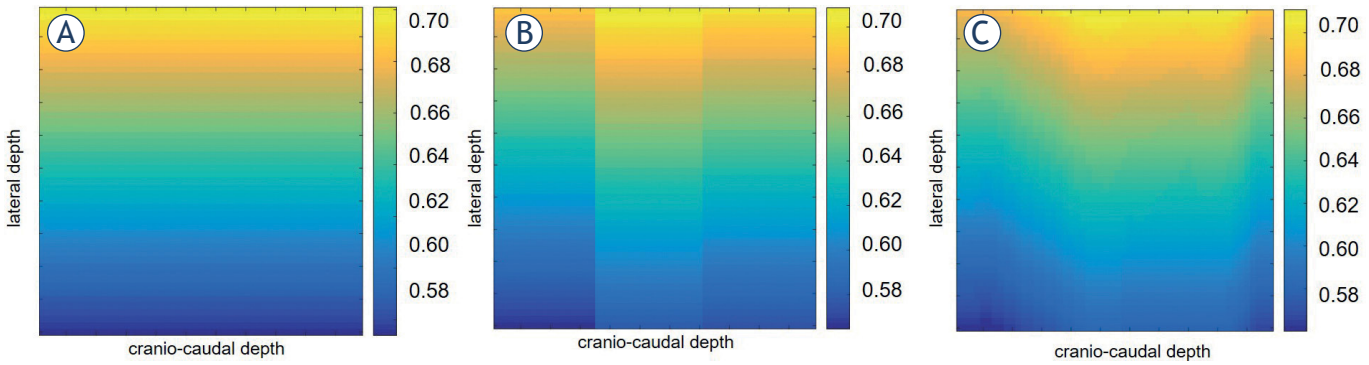

FIGURE 5. Optimal fluence maps from **(A)** assuming a single penetration depth, from **(B)** assuming a three-region breast model, and **(C)** our proposed model. Colorbar shows beam fluence.

Average percent difference and average distance in cm between the automatic-algorithm-measured and hand-measured breast radius and separation over the three test volumes can be found in Table 1. Average percent difference between the breast radius measurements over the three test volumes was 12.6% (95% confidence interval 10.4% – 14.8%), corresponding to an actual measurement error of 0.69 cm (0.59 cm – 0.79 cm). Average percent difference between the breast separation measurements over the three test volumes was 5.2% (95% confidence interval 5.1% – 5.3%), corresponding to an actual measurement error of 0.92 cm (0.79 cm – 1.05 cm). It should be noted that the reconstructed voxel size was 1.269 mm, hence these errors are below 8 pixels at a measurement error value of 1 cm.

Figure 4 displays the correlation between the breast separation and radius with the optimal transmission fluence at the breast surface needed to deliver the most homogenous dose distribution to the breast volume using a 6 MV x-ray beam. This plot indicates an increase in the x-ray fluence needed as the breast separation decreases and the radius increases. Following the fitting of a plane to the model, the relationship in Equation 2 was acquired, where *f* is the optimal fluence for the axial slice with a radius and separation measurement from the semi-supervised framework.

[eq. 2] $f\,(radius, separation, 6\ MV) = 0.753 + 0.006 * radius - 0.005 * separation$

These results are in agreement with the work of Emmens[11] and Alghufaili[16], which reported correlation between a decreasing separation and an increase in radius with the TPD. The TPD is related with x-ray fluence, in that more fluence is needed to attain a deeper penetration depth. The mathematical relationship between breast size and shape and the optimal fluence for a 23 MV beam can be found in Equation 3. To simplify the number of parameters in the Equation and improve the generalizability of the model, we assumed a bilinear fit for each of the three models.

[eq. 3] $f\,(radius, separation, 23\ MV) = 0.888 + 0.006 * radius - 0.007 * separation$

Figure 5 shows optimal fluence maps generated using a single TPD throughout the treatment volume, using three TPDs assuming a three-region

TABLE 2. Summary of dose homogeneity indices (HI) for all ten collected treatment courses. Compared are the treatments generated with our proposed algorithm, plans created using the 3-region breast model proposed by Alghufaili, those plans optimized by a medical dosimetrist, and plans generated by assuming a single transmission penetration depth (TPD) within the treatment planning software

Number	Proposed Work HI	3-region breast model	Dosimetrist Optimized HI	Single TPD HI
1	26.7	22.4	16.5	23.0
2	17.8	19.2	14.1	19.1
3	10.6	15.2	11.2	17.2
4	11.8	14.6	9.51	13.3
5	8.49	7.87	3.32	8.04
6	8.79	14.1	6.64	12.6
7	4.59	7.44	3.82	8.19
8	7.57	21.5	8.84	23.5
9	11.3	17.9	8.29	18.7
10	10.6	16.0	10.5	17.8
Average	**12.6**	**15.6**	**9.87**	**17.0**

TABLE 3. Summary of global dose maximum and clinical target volume (CTV) minimum values for all ten collected treatment courses. Compared are the treatments generated with our proposed algorithm, plans created using the 3-region breast model proposed by Alghufaili, those plans optimized by a medical dosimetrist, and plans generated by assuming a single transmission penetration depth (TPD) within the treatment planning software

	Global dose max (%)				CTV dose min (%)			
Number	Proposed work	3-region breast model	Dosimetrist optimized	Single TPD	Proposed work	3-region breast model	Dosimetrist optimized	Single TPD
1	107.7	108.5	109.1	113.3	96.9	97.3	104.1	96.0
2	109.7	111.3	106.5	111.8	74.4	75.0	76.9	74.2
3	107.4	108.1	107.5	112.7	95.5	88.7	95.3	89.1
4	107.5	110.4	105.9	109.8	95.5	95.2	95.0	96.8
5	107.7	109.7	104.0	105.0	95.1	95.9	98.1	87.8
6	107.5	108.7	105.5	111.4	97.9	96.0	99.3	97.4
7	108.0	114.2	105.9	116.3	95.4	95.4	95.7	95.4
8	107.6	112.6	106.6	114.6	95.3	92.8	97.8	94.1
9	107.5	115.5	106.0	118.1	95.6	95.6	95.1	95.0
10	107.5	108.6	107.8	114.4	86.1	81.6	87.8	87.2
Average	**107.8**	**111.2**	**106.5**	**112.7**	**92.7**	**91.4**	**94.5**	**91.3**

TABLE 4. Summary of mean dose to the heart and ipsilateral lung V20 Gy for all ten collected courses. Compared are the treatments generated with our proposed algorithm, plans created using the 3-region breast model proposed by Alghufaili, those plans optimized by a medical dosimetrist, and plans generated by assuming a single transmission penetration depth (TPD) within the treatment planning software

	Mean dose to the heart (cGy)				Ipsilateral lung $V_{20\,Gy}$ (%)			
Number	Proposed Work	3-region breast model	Dosimetrist Optimized	Single TPD	Proposed Work	3-region breast model	Dosimetrist Optimized	Single TPD
1	11.0	15.0	13.7	13.4	0.42	2.30	2.41	2.05
2	298	296	294	327	18.2	18.3	16.7	20.3
3	177	165	109	160	5.12	4.91	3.56	4.65
4	271	267	149	250	9.09	9.03	8.07	7.93
5	40.8	44.9	39.7	42.0	16.6	16.8	15.8	16.2
6	113	112	108	111	8.95	8.84	8.33	8.59
7	47.0	52.4	47.7	51.7	9.56	11.2	9.9	10.9
8	26.9	28.9	26.5	28.7	11.4	11.2	11.4	10.9
9	95.9	128	89.5	125	9.18	10.8	7.8	10.6
10	406	402	159	397	18.7	18.5	12.4	18.2
Average	**149**	**151**	**104**	**151**	**10.7**	**11.2**	**9.65**	**11.0**

breast model, and using a different TPD for each slice throughout the treatment volume. It should be noted that the resolution of these maps is consistent with that of the imaging (1.269 mm).

Table 2 summarizes the HI for each of the collected ECOMP plans comparing the original medical dosimetrist plans, plans from our proposed algorithm, plans generated using the 3-region breast model proposed by Alghufaili, and plans from the use of a single TPD over the entire treatment volume. Over the collected plans, there is no statistical difference between the medical dosimetrist plans and our algorithm's plans in terms of the dose homogeneity index. Table 3 summarizes the global

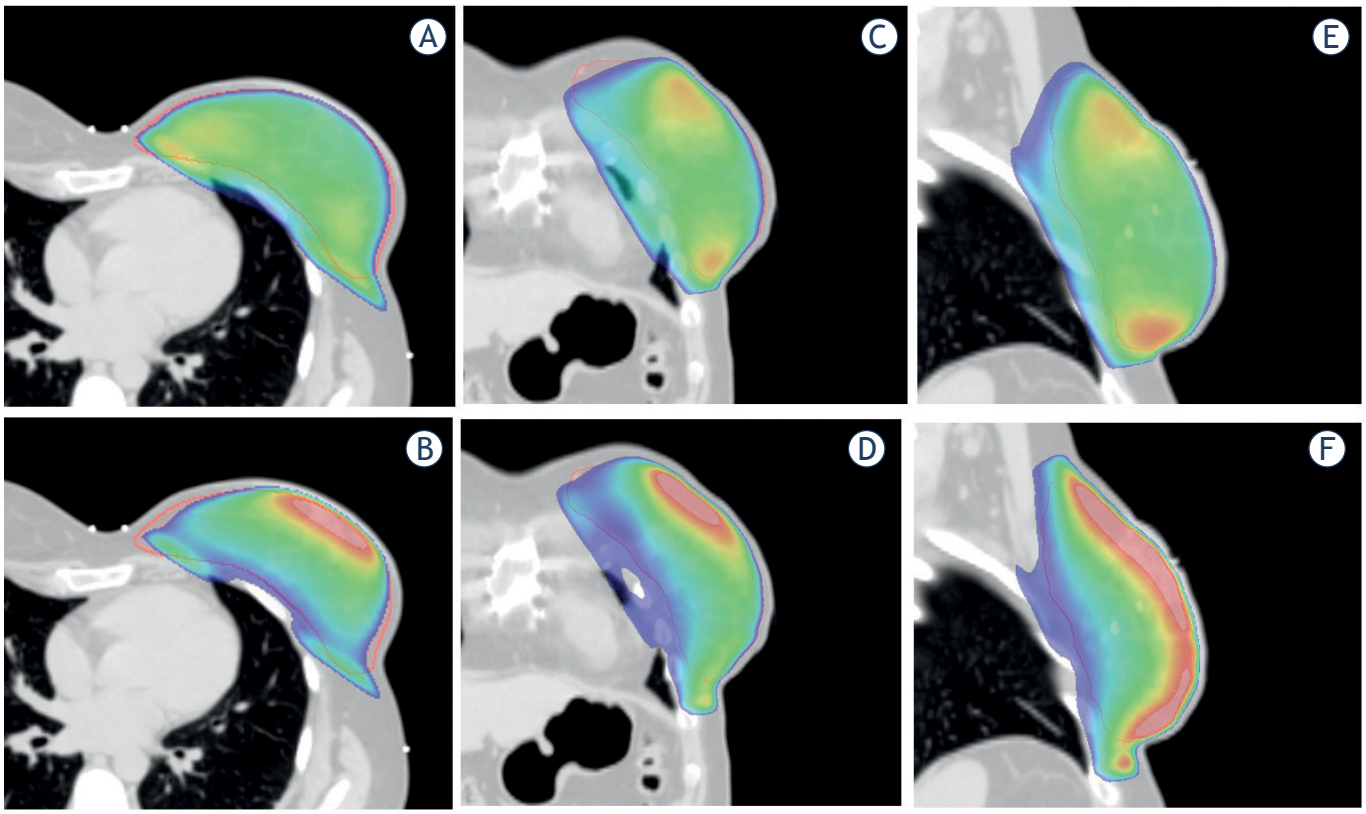

FIGURE 6. (A, C, E) axial, coronal, and sagittal views of the breast treatment volume showing the isodose color washes from the treatment plan generated with the proposed algorithm. **(B, D, F)** axial, coronal, and sagittal views of the breast treatment volume showing the isodose color washes from the treatment plan generated by assuming a constant transmission penetration depth of 30%.

dose maximum and treatment volume dose minimum for each of the 10 collected plans. Compared with the use of a single TPD, our algorithm is able to generate fluence maps which yield global maximum doses and treatment volume dose minimums that are within our institution's constraints that is in better agreement with the medical dosimetrist plans. Table 4 summarizes the mean dose to the heart and summarizes the volume percent above 20 Gy for the ipsilateral lung ($V_{20\ Gy}$) over the 10 collected plans. There is no statistical difference between the medical dosimetrist plans and our algorithm plans in terms of the heart mean dose or the ipsilateral lung $V_{20\ Gy}$.

Figure 6 demonstrates isodose color washes in the axial, sagittal, and coronal planes, one set generated from fluence maps generated with our proposed algorithm, the other from the current model utilized in the Eclipse TPS that assumes a constant TPD over the entire treatment volume. Our proposed algorithm creates a plan that has more homogenous coverage of the breast and a reduced anterior hotspot. This specific case had a HI of 10.6 from the plan generated using our proposed algorithm and 17.2 from the plan assuming a constant TPD of 30% throughout the breast volume. Using the 3-region breast model to generate the treatment plan yielded an HI of 15.2.

Discussion

This study proposed a semi-supervised scheme for the determination of the optimal x-ray fluence map needed to deliver the most homogenous dose distribution to the breast volume in ECOMP treatment plans. Our algorithm takes as input the CT-simulation data from pre-treatment imaging and

uses the breast radius and separation measurement over the entire treatment volume to output tangential maps of the x-ray fluence that describes how to deliver the most homogenous dose profiles such that acute late effects due to radiation toxicity caused by radiation dose in-homogeneities can be reduced. This fluence determination takes into consideration the variation in breast separation and radius in the cranio-caudal direction, and extends on previous work by using each axial slice in the volume to optimize the homogeneity instead of just a single or a couple slices. Figures 1, 2, and 5 emphasize the importance in considering this variation in the size and shape of the breast in the cranio-caudal direction. The three fluence maps in Figure 5 show how the optimal fluence maps change when the breast is broken up into finer resolution sections, from a single uniform shape in Figure 5A, three uniform shapes in Figure 5B, to estimating the exact shape at each axial slice in Figure 5C. Our results indicate that the proposed algorithm can create plans that are statistically non-inferior in terms of the dose homogeneity to those plans manually edited by a dosimetrist. Additionally, our algorithm is able to produce plans that are within our institution's dose constraints for the global dose maximum and target dose minimum.

A comparison of the isodose color washes in Figure 6 show a better coverage of the green color wash over more of the treatment volume when the proposed algorithm is used instead of a constant TPD of 30%. In the axial slice (Figure 6 A and 6B), the green wash extends closer to the posterior edge of the breast volume against the lung volume. The sagittal view (Figure 6E and 6F) shows an advantage to our proposed algorithm in the coverage of the green wash towards the inferior portion of the breast volume. In all three anatomical planes, the green wash is more homogenous throughout the treatment volume, as confirmed with the homogeneity index for this specific case (10.6 for the proposed algorithm, 17.2 for the constant TPD). There is also a reduction in the anterior hot spot that is prevalent in all three of the views from the single TPD treatments.

The mathematical models fitted for the 6 MV and 23 MV beams (Equations 2 & 3, respectively), are both dominated by the 0^{th} degree additive constant. The breast radius and separation play a role (additive for the radius, subtractive for the separation), but it is small.

With breasts of small radius and separation, our semi-supervised size measurement algorithm tends to overestimate the radius and separation of the breast, thereby generating plans that have regions where the dose potentially would exceed the maximum dose constraint. It would be these cases where manual optimization by the medical dosimetrist would still be necessary to reduce the hotspots potentially present in the dose profile. Patients 1 and 5 in Table 2 are examples of this. They both had overestimations in the breast radius and separation, causing the homogeneity to be worse compared with the medical dosimetrist plans due to the presence of several local dose hotspots that didn't go above the 108% global maximum dose constraint, but still reduced homogeneity.

This work can be thought of as a more homogenous starting point for the iterative optimization process of the medical dosimetrist. Currently, a single TPD is empirically selected within Eclipse and the resultant fluence maps are manually edited to improve the homogeneity of the computed dose profiles to bring the plan within institutional dose constraints. Our work has shown that an algorithm that measures the breast separation and radius over the entire breast volume and relates them to the optimal x-ray fluence maps can lead to more homogenous plans than the use of a single TPD. It seems possible that these improvements were realized with the higher-resolution correlation of breast size and shape to the x-ray beam fluence. This work may lead to a quicker, less manually intensive process for the dosimetrist to bring the ECOMP plans within dose constraints. In every collected case, some combination of the global dose maximum being too high or treatment volume minimum dose being too low led to the necessity of optimization of the single TPD plans by the dosimetrist. In the cases that met dose constraints with dosimetrist editing, our algorithm was able to create plans that met dose constraints with no manual editing required. There still may be manual editing required to achieve equivalent dose homogeneity with the dosimetrist-edited plans, however compared with the use of a single TPD or a three-region breast model, the plans from our algorithm attain a higher level of homogeneity and are more deliverable when considering institutional dose constraints.

Our work extends on the literature in this problem space in several important ways. Firstly, our work accounts for the variation in breast radius and separation in the cranio-caudal direction, axial slice by axial slice, by estimating the breast radius and separation at each slice and correlating it with the optimal (in terms of beam homogeneity) beam penetration using the TPD value. Secondly,

we took this TPD value and determined a mathematical model, which governed what beam fluences would be needed to deliver parallel-opposed beams of the prescribed TPD. In this manner, the TPS would not be needed to obtain the optimized x-ray fluence map.

A limitation of this current work is our model assumes exponential drop-off of the beam governed by the Beer-Lambert-Bouguer Law. This assumes a homogenous material that the x-rays are traveling through, and will not be the case in the breast volume. This may cause the assumed fluences to not be exactly what would be achieved with the delivery of a particular TPD deemed optimal for the breast separation and radius slice-by-slice. An additional limitation is in cases where there is skin folding at the breast surface, as may occur in the case of a large, pendulous breast. A challenging situation is created in that the breast radius and separation would not be impacted, yet the optimal TPD and x-ray fluence would be changed. Such a condition was not included in the development of our model, so it may lead to the creation of suboptimal plans. One final limitation is at this point, our algorithm still requires an operator for medial and ipsilateral marker identification. The supervision amount is low compared to the current clinical workflow, however a fully automated framework would improve the clinical applicability of this algorithm.

Conclusions

This work indicates the advantages to the consideration of the full volumetric shape of the breast to determine the optimal TPD needed to deliver a homogenous dose distribution to the breast treatment volume. This volumetric shape is defined by the measurement of the breast separation along the posterior edge and radius from the isocenter at the posterior border to the apex anteriorly, considering all axial slices in the cranio-caudal direction. This work also detailed a method for the semi-supervised determination of this volumetric shape, resulting in the output of the x-ray fluence needed for the delivery of the optimal dose distribution. We envision this process used to attain a more homogenous, consistent starting point for the medical dosimetrist as they optimize the ECOMP treatment plans, compared with assuming a constant shape of the breast in the cranio-caudal direction.

References

1. American Cancer Society I. *Breast Cancer Facts & Figures 2019-2020.* Atlanta; 2019.
2. Aref A, Thornton D, Youssef E, He T, Tekyi-Mensah S, Denton L, et al. Dosimetric improvements following 3D planning of tangential breast irradiation. *Int J Radiat Oncol Biol Phys* 2000; **5:** 1569-74. doi: 10.1016/S0360-3016(00)00808-7
3. Donovan EM, Johnson U, Shentall G, Evans PM, Neal AJ, Yarnold JR. Evaluation of compensation in breast radiotherapy: a planning study using multiple static fields. *Int J Radiat Oncol Biol Phys* 2000; **3:** 671-9. doi: 10.1016/S0360-3016(99)00388-0
4. Kestin LL, Sharpe MB, Frazier RC, Vicini FA, Yan D, Matter RC, et al. Intensity modulation to improve dose uniformity with tangential breast radiotherapy: initial clinical experience. *Int J Radiat Oncol Biol Phys* 2000; **5:** 1559-68. doi: 10.1016/S0360-3016(00)01396-1
5. Correa CR, Litt HI, Hwang W-T, Ferrari VA, Solin LJ, Harris EE. Coronary artery findings after left-sided compared with right-sided radiation treatment for early-stage breast cancer. *J Clin Oncol* 2007; **21:** 3031-7. doi: 10.1200/JCO.2006.08.6595
6. Harris EER, Correa C, Hwang W-T, Liao J, Litt HI, Ferrari VA, et al. Late cardiac mortality and morbidity in early-stage breast cancer patients after breast-conservation treatment. *J Clin Oncol* 2006; **25:** 4100-6. doi: 10.1200/JCO.2005.05.1037
7. Recht A. Which breast cancer patients should really worry about radiation-induced heart disease – and how much? *J Clin Oncol* 2006; **25:** 4059-61. doi: 10.1200/JCO.2006.07.7909
8. Goldsmith C, Haviland J, Tsang Y, Sydenham M, Yarnold J. Large breast size as a risk factor for late adverse effects of breast radiotherapy: Is residual dose inhomogeneity, despite 3D treatment planning and delivery, the main explanation? *Radiother Oncol* 2011; **2:** 236-40. doi: 10.1016/j.radonc.2010.12.012
9. Moody AM, Mayles WPM, Bliss JM, A'Hern RP, Owen JR, Regan J, et al. The influence of breast size on late radiation effects and association with radiotherapy dose inhomogeneity. *Radiother Oncol* 1994; **2:** 106-12. doi: 10.1016/0167-8140(94)90063-9
10. Chui CS, Hong L, Hunt M, McCormick B. A simplified intensity modulated radiation therapy technique for the breast. *Med Phys* 2002; **4:** 522-9. doi: 10.1118/1.1460875
11. Emmens D, James H. Irregular surface compensation for radiotherapy of the breast: correlating depth of the compensation surface with breast size and resultant dose distribution. *Brit J Radiol* 2010; **986:** 159-65. doi: 10.1259/bjr/65264916
12. James H, Poynter A, Crosbie J, MacKenzie L, Boston S, LeVay J. Electronic compensation for CT planned breast treatments. *Radiother Oncol* 2002; S133-4.
13. James H, Scrase C, Poynter A. Practical experience with intensity-modulated radiotherapy. *Brit J Radiol* 2004; **913:** 3-14. doi: 10.1259/bjr/14996943
14. LeVay J, James H, Poynter A, MacKenzie L, Boston S. Optimising the delivery of radiotherapy for early breast cancer by the use of IMRT. *Clin Oncol* 2003; S14.
15. Friend M. An overview of electronic tissue compensation (ECOMP) for breast radiotherapy. *2014 Combined Scientific Meeting*. Vienna, Austria; 2014.
16. Alghufaili AH, Shanmugarajah L, Kumaraswamy LK. Correlating the depth of compensation to the 3-D shape of the breast to achieve homogeneous dose distribution using the electronic tissue compensation treatment technique. *Med Dosim* 2019; **1:** 30-4. doi: 10.1016/j.meddos.2018.01.001
17. Xie Y, Ji Q. A new efficient ellipse detection method. In: *Object recognition supported by user interaction for service robots*. Troy, New York: IEEE, Rensselaer Polytechnic Institute; 2002. doi: 10.1109/ICPR.2002.1048464
18. Beer A. Bestimmung der absorption des rothen lichts in farbigen flussigkeiten. *Ann Physik* 1852; 78-88. doi: 10.1002/andp.18521620505
19. Bouguer P. Essai d'optique sur la gradation de la lumière. chez Claude Jombert, ruë S. Jacques, au coin de la ruë des Mathurins, à l ...; 1729

20. Lambert JH. *Photometria sive de mensura et gradibus luminis, colorum et umbrae.* Augsburg: Christoph Peter Detleffsen for the widow of Eberhard Klett; 1760

21. Wu Q, Mohan R, Morris M, Lauve A, Schmidt-Ullrich R. Simultaneous integrated boost intensity-modulated radiotherapy for locally advanced head-and-neck squamous cell carcinomas. I: dosimetric results. *Int J Radiat Oncol Biol Phys* 2003; **56:** 573-85. doi: 10.1016/s0360-3016(02)04617-5

22. Koo TK, Li MY. A guideline of selecting and reporting intraclass correlation coefficients for reliability research. *J Chiropr Med* 2016; **2:** 155-63. doi: 10.1016/j.jcm.2016.02.012